nature neuroscience

Cellular origins of auditory event-related potential deficits in Rett syndrome

Darren Goffin[1], Edward S Brodkin[2], Julie A Blendy[3], Steve J Siegel[2] & Zhaolan Zhou[1]

Dysfunction in sensory information processing is a hallmark of many neurological disorders, including autism spectrum disorders, schizophrenia and Rett syndrome (RTT). Using mouse models of RTT, a monogenic disorder caused by mutations in *MECP2*, we found that the large-scale loss of MeCP2 from forebrain GABAergic interneurons led to deficits in auditory event-related potentials and seizure manifestation, whereas the restoration of MeCP2 in specific classes of interneurons ameliorated these deficits.

Sensory information processing, the ability to accurately interpret and convert environmental stimuli into appropriate thoughts and decisions, represents a core domain of social behavior and cognitive function[1]. Despite diverse genetic etiologies, deficits in sensory information processing, measured as changes in auditory or visual event-related potentials (ERPs), represent an endophenotype commonly shared among patients with RTT, autism spectrum disorders (ASDs) and schizophrenia[1–3]. Similar deficits in ERPs are also observed in mouse models of RTT concomitant with the manifestation of behavioral abnormalities[4,5]. However, the cellular origins and neural mechanisms underlying ERP deficits are poorly understood.

We sought to dissect the causally important alterations in neural circuits and cellular origins of auditory ERP deficits in mouse models of RTT. We bred mice with *loxP*-flanked *Mecp2* (*Mecp2*$^{2lox/+}$)[6] with mice expressing Cre recombinase under the control of either the *Dlx5/6* enhancer to remove MeCP2 from forebrain GABAergic neurons[7] or the *Emx1* promoter to remove MeCP2 from forebrain glutamatergic neurons and glia[8] (**Fig. 1a**). We then examined ERPs by recording hippocampal local field potential (LFP) responses to auditory events consisting of white noise pips in awake, freely mobile mice. *Mecp2*$^{2lox/y}$ mice exhibited a stereotypical decrease in event-related power at low frequencies and an increase in event-related power at high frequencies, similar to previous findings[4] (**Fig. 1b**,**c**). We also observed a robust increase in phase-locking factor (PLF), a measure of trial-to-trial reliability, across all frequencies (**Supplementary Fig. 1**). In contrast, *Mecp2*$^{2lox/y}$*; Dlx5/6-cre* mice exhibited a marked and significant reduction in event-related power and PLF responses across all frequencies relative to *Mecp2*$^{2lox/y}$ mice (permutation test with FDR < 0.05; **Fig. 1b**,**c** and **Supplementary Fig. 1**). These alterations were not the result of altered hearing, as auditory brainstem responses, an evoked measure of activity in the brainstem used to assess hearing in humans and mice[9], were unaffected (**Supplementary Fig. 2**).

In comparison, *Mecp2*$^{2lox/y}$*; Emx1-cre* mice, which lack MeCP2 in forebrain glutamatergic neurons and glia, exhibited auditory-evoked power and PLF responses that were indistinguishable from those observed in *Mecp2*$^{2lox/y}$ littermates (**Fig. 1a**,**b** and **Supplementary Fig. 1**). Basal oscillations in the high-frequency range, however, were elevated in mice lacking MeCP2 from either glutamatergic or GABAergic neurons, similar to that observed in *Mecp2*-null mice[4] (**Supplementary Fig. 3**). Given that *Dlx5/6-cre* exhibits recombination in forebrain GABAergic interneurons and striatal medium spiny neurons (MSNs)[7,10], we next conditionally deleted MeCP2 from either D1 or D2 dopamine receptor–expressing MSNs[11]. We found that auditory-evoked power and PLF were unaffected by loss of MeCP2 from either population of MSNs (**Supplementary Fig. 4**). Thus, these data suggest that loss of MeCP2 from forebrain GABAergic interneurons is primarily responsible for the observed deficits in auditory ERPs in mouse models of RTT.

Previous work found that loss of MeCP2 from forebrain GABAergic neurons results in motor incoordination, ataxia and altered social interactions[12]. In contrast, we found that *Mecp2*$^{2lox/y}$*; Emx1-cre* mice exhibited a significant decrease in locomotor activity ($P = 0.043$, two-tailed *t* test with Welch's correction), but no substantial alterations in motor coordination on an accelerating rotarod, anxiety-like behavior, social interactions, or episodic learning and memory (**Supplementary Fig. 5**). Thus, MeCP2 in the forebrain appears to be critical for motor control, but auditory ERPs and social behaviors are particularly sensitive to MeCP2 function in forebrain GABAergic neurons.

Seizures represent one of the most debilitating symptoms in RTT[13]. However, mouse models of RTT show few, if any, behavioral seizures. We found that *Mecp2*$^{2lox/y}$*; Dlx5/6-cre* mice frequently exhibited behavioral seizures that were recurring and lasted 10–60 s following routine handling of the mice after 3 months of age (**Fig. 1d** and **Supplementary Videos 1–3**). Electroencephalographic (EEG) recordings revealed electrographic seizures consisting of 6–8-Hz spikes and wave discharges (SWDs) that were associated with behavioral arrest in *Mecp2*$^{2lox/y}$*; Dlx5/6-cre* mice (**Fig. 1e**). In contrast, we did not detect behavioral or electrographic seizures in *Mecp2*$^{+/y}$, *Mecp2*$^{2lox/y}$ or *Mecp2*$^{2lox/y}$*; Emx1-cre* mice despite prolonged monitoring at these ages. Together, these data suggest that the loss of MeCP2 from forebrain GABAergic neurons leads to hyperexcitability, which manifests as seizures.

We next examined whether the preservation of MeCP2 function in forebrain GABAergic neurons is sufficient to maintain normal auditory ERPs in otherwise *Mecp2*-null mice. We bred *Dlx5/6-cre* and *Emx1-cre* mice with mice containing a *loxP*-flanked transcriptional Stop

[1]Department of Genetics, Perelman School of Medicine, University of Pennsylvania, Philadelphia, Pennsylvania, USA. [2]Department of Psychiatry, Perelman School of Medicine, University of Pennsylvania, Philadelphia, Pennsylvania, USA. [3]Department of Pharmacology, Perelman School of Medicine, University of Pennsylvania, Philadelphia, Pennsylvania, USA. Correspondence should be addressed to Z.Z. (zhaolan@mail.med.upenn.edu).

Received 28 January; accepted 31 March; published online 28 April 2014; doi:10.1038/nn.3710

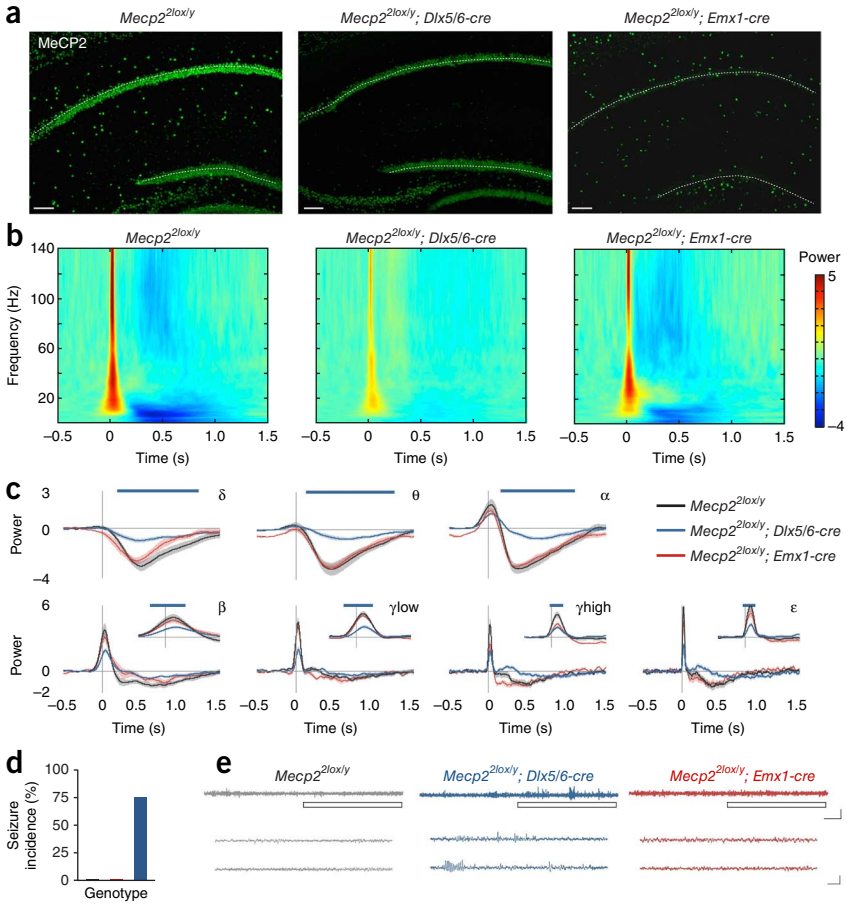

Figure 1 MeCP2 function in forebrain GABAergic, but not glutamatergic neurons, is necessary for auditory ERPs. (**a**) MeCP2 immunoreactivity in the hippocampus of *Mecp2*$^{2lox/y}$ mice and those in which MeCP2 was conditionally deleted from forebrain GABAergic (*Mecp2*$^{2lox/y}$*; Dlx5/6-cre*) or glutamatergic neurons (*Mecp2*$^{2lox/y}$*; Emx1-cre*). Glutamatergic pyramidal and granule cell layers are marked by dotted white lines. Scale bars represent 100 μm. These localization patterns were observed in three mice per genotype. (**b**) Heat maps showing changes in event-related power in response to 85-dB white noise sound presentation as a function of time and frequency. (**c**) Population averages of event-related power separated into frequency bands (δ, 2–4 Hz; θ, 4–8 Hz; α, 8–12 Hz; β, 12–30 Hz; γlow, 30–50 Hz; γhigh, 50–90 Hz; ε, 90–140 Hz) for *Mecp2*$^{2lox/y}$*; Dlx5/6-cre* mice ($n = 13$), *Mecp2*$^{2lox/y}$*; Emx1-cre* mice ($n = 7$) and *Mecp2*$^{2lox/y}$ mice ($n = 9$). Shaded regions represent s.e.m. Top blue bars represent those regions with FDR < 0.05 (permutation test). (**d**) The percentage of mice exhibiting behavioral seizures (**Supplementary Videos 1–4**). (**e**) Top, representative EEG traces from awake, freely mobile mice. Scale bars represent 5 s (horizontal) and 200 μV (vertical). Bottom traces are expanded views taken from boxed regions. Scale bars represent 1 s (horizontal) and 200 μV (vertical).

sequence in the endogenous *Mecp2* gene (*Mecp2*^{Stop})[14]. We confirmed that MeCP2 was expressed in the majority of GAD67-expressing neurons in *Mecp2*$^{Stop/y}$*; Dlx5/6-cre*, but not *Mecp2*$^{Stop/y}$*; Emx1-cre*, mice (**Supplementary Fig. 6**). Similar to our previous studies in *Mecp2*-null mice[4], we found that auditory-evoked neural responses were markedly and significantly reduced in *Mecp2*$^{Stop/y}$ mice compared with their *Mecp2*$^{+/y}$ littermates (permutation test, FDR < 0.05; **Fig. 2** and **Supplementary Fig. 7**). Recordings in *Mecp2*$^{Stop/y}$*; Dlx5/6-cre*, but not *Mecp2*$^{Stop/y}$*; Emx1-cre*, mice revealed a significant preservation of auditory-evoked power and PLF compared with *Mecp2*$^{Stop/y}$ mice (permutation test, FDR < 0.05; **Fig. 2** and **Supplementary Fig. 7**). Furthermore, *Mecp2*$^{Stop/y}$*; Emx1-cre* mice, in which MeCP2 expression is preserved in most forebrain neurons and glia except GABAergic neurons, showed behavioral seizures around 2 months of age (**Supplementary Video 4**). Notably, the marked RTT-like phenotypes and decreased longevity in *Mecp2*$^{Stop/y}$ mice were not rescued by selective preservation of MeCP2 in forebrain glutamatergic or GABAergic neurons (**Supplementary Fig. 8**), which is likely a result of the absence of MeCP2 from mid- and hindbrain regions that control respiration and autonomic function[12,15]. Together, these results suggest that MeCP2 function in forebrain GABAergic neurons is required for maintaining proper auditory ERPs and preventing seizure manifestation.

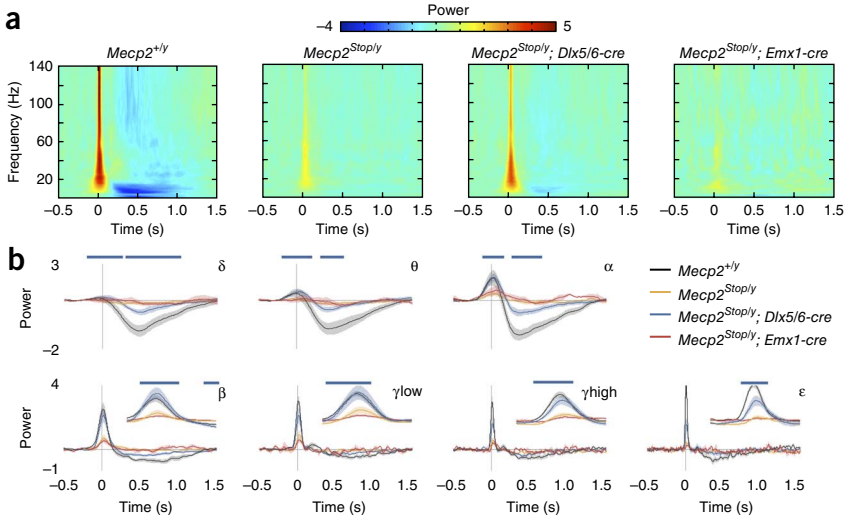

Figure 2 Preservation of MeCP2 function in forebrain GABAergic neurons restores auditory ERPs in *Mecp2*-null mice. (**a**) Heat maps showing changes in event-related power in response to 85-dB white noise sound presentation as a function of time and frequency. (**b**) Population averages of event-related power for *Mecp2*$^{Stop/y}$*; Dlx5/6-cre* ($n = 11$), *Mecp2*$^{Stop/y}$*; Emx1-cre* ($n = 6$), *Mecp2*$^{Stop/y}$ mice ($n = 9$) and *Mecp2*$^{+/y}$ mice ($n = 9$). Frequency bands correspond to: δ, 2–4 Hz; θ, 4–8 Hz; α, 8–12 Hz; β, 12–30 Hz; γlow, 30–50 Hz; γhigh, 50–90 Hz; ε, 90–140 Hz. Shaded regions represent s.e.m. Top blue line represents those regions with FDR < 0.05 (permutation test).

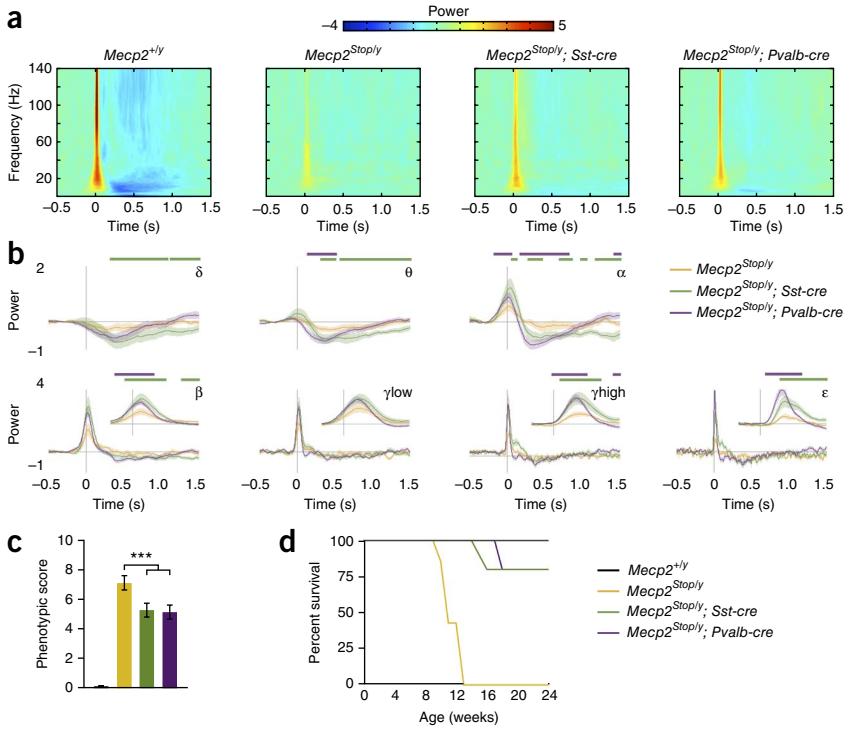

Figure 3 Preservation of MeCP2 function in either SOM- or PV-expressing interneurons leads to a partial restoration of auditory ERPs. (**a**) Heat maps showing changes in event-related power in response to 85-dB white noise sound presentation as a function of time and frequency. (**b**) Population averages of event-related power for *Mecp2*$^{Stop/y}$*; Pvalb-cre* ($n = 7$), *Mecp2*$^{Stop/y}$*; Sst-cre* ($n = 12$) and *Mecp2*$^{Stop/y}$ mice ($n = 9$). Frequency bands correspond to: δ, 2–4 Hz; θ, 4–8 Hz; α, 8–12 Hz; β, 12–30 Hz; γlow, 30–50 Hz; γhigh, 50–90 Hz; ε, 90–140 Hz. Shaded regions represent s.e.m. Top green or purple bars represent those regions with FDR < 0.05 (permutation test) in *Sst-cre* or *Pvalb-cre*, respectively. (**c**) Phenotypic scoring of mice at 12 weeks of age ($n = 8$ per genotype). ***$P < 0.001$, one-way ANOVA with *post hoc* Tukey. Bars represent mean ± s.e.m. (**d**) Survival curves for mice ($n = 8$ per genotype).

To further evaluate the GABAergic interneuron cell types mediating these effects, we examined the contributions of MeCP2 in parvalbumin (PV, *Pvalb*)- and somatostatin (SOM, *Sst*)-expressing interneurons by conditionally deleting MeCP2 from PV- or SOM-expressing interneurons using the *Pvalb-cre*[16] and *Sst-cre*[17] mouse lines. We found that auditory-evoked power and PLF (**Supplementary Fig. 9**) in *Mecp2*$^{2lox/y}$*; Pvalb-cre* or *Mecp2*$^{2lox/y}$*; Sst-cre* mice were indistinguishable from that of their *Mecp2*$^{2lox/y}$ littermates. In addition, we did not observe any behavioral seizures, overt RTT-like abnormalities or decreased longevity in these mice. Notably, however, we found that the selective preservation of MeCP2 in either PV- or SOM-expressing interneurons led to a significant preservation of auditory-evoked power and PLF compared with *Mecp2*$^{Stop/y}$ mice (permutation test, FDR < 0.05; **Fig. 3a,b** and **Supplementary Fig. 10**). Previous work suggests that soma-targeting PV interneurons regulate the output firing of pyramidal neurons, whereas the dendrite-targeting SOM-expressing interneurons modulate the input to these neurons[18–20]. Restoring MeCP2 function in either PV- or SOM-expressing interneurons may therefore be sufficient to partially restore proper neural network activity and thereby help to stabilize auditory ERPs. Preservation of MeCP2 in either PV- or SOM-expressing interneurons also ameliorated overt RTT-like behavioral phenotypes ($P < 0.001$, one-way ANOVA with *post hoc* Tukey test; **Fig. 3c**) and prolonged longevity in *Mecp2*$^{Stop/y}$ mice (**Fig. 3d**). This is likely a result of the restored expression of MeCP2 in PV or SOM interneurons that are widely distributed throughout the brain.

In summary, our findings demonstrate that MeCP2 function in forebrain GABAergic, but not glutamatergic, neurons is required for generating auditory ERPs. In addition, loss of MeCP2 function in GABAergic neurons by either ablation of MeCP2 from GABAergic neurons or preservation of MeCP2 in glutamatergic neurons in *Mecp2*-null mice led to cortical hyperexcitability and behavioral seizures. Furthermore, we found that deficits in auditory ERPs occurred following the large-scale loss of MeCP2 from forebrain GABAergic interneurons; but restoration of MeCP2 function in either PV- or SOM-expressing interneurons was able to ameliorate these deficits. Thus, our findings provide a platform for exploring these differential cellular influences on ERPs and for developing new therapeutic strategies to alleviate sensory information processing impairments in ASDs, schizophrenia and RTT.

METHODS

Methods and any associated references are available in the online version of the paper.

Note: Any Supplementary Information and Source Data files are available in the online version of the paper.

ACKNOWLEDGMENTS

We thank members of the Zhou laboratory for critical reading of the manuscript. This work was supported by US National Institutes of Health grants R01 NS081054 and R01 MH091850 (Z.Z.) and the International Rett Syndrome Foundation (Z.Z. and D.G.). Z.Z. is a Pew Scholar in Biomedical Sciences.

AUTHOR CONTRIBUTIONS

D.G. and Z.Z. designed the experiments and wrote the manuscript. D.G. conducted the experiments and performed data analysis. E.S.B. and J.A.B. helped to design and interpret the behavioral tests. S.J.S. helped to design and interpret the electrophysiology studies.

COMPETING FINANCIAL INTERESTS

The authors declare no competing financial interests.

1. Uhlhaas, P.J. & Singer, W. *Neuron* **75**, 963–980 (2012).
2. Chahrour, M. & Zoghbi, H.Y. *Neuron* **56**, 422–437 (2007).
3. Goffin, D. & Zhou, Z. *Front. Biol.* **7**, 428–435 (2012).
4. Goffin, D. *et al. Nat. Neurosci.* **15**, 274–283 (2012).
5. Liao, W. *et al. Neurobiol. Dis.* **46**, 88–92 (2012).
6. Chen, R.Z., Akbarian, S., Tudor, M. & Jaenisch, R. *Nat. Genet.* **27**, 327–331 (2001).
7. Monory, K. *et al. Neuron* **51**, 455–466 (2006).
8. Gorski, J.A. *et al. J. Neurosci.* **22**, 6309–6314 (2002).
9. Hardisty-Hughes, R.E., Parker, A. & Brown, S.D.M. *Nat. Protoc.* **5**, 177–190 (2010).
10. Zhao, Y.-T., Goffin, D., Johnson, B. & Zhou, Z. *Neurobiol. Dis.* **59**, 257–266 (2013).
11. Gong, S. *et al. J. Neurosci.* **27**, 9817–9823 (2007).
12. Chao, H.-T. *et al. Nature* **468**, 263–269 (2010).
13. Katz, D.M. *et al. Dis. Model. Mech.* **5**, 733–745 (2012).
14. Guy, J., Gan, J., Selfridge, J., Cobb, S. & Bird, A. *Science* **315**, 1143–1147 (2007).
15. Ward, C.S. *et al. J. Neurosci.* **31**, 10359–10370 (2011).
16. Madisen, L. *et al. Nat. Neurosci.* **13**, 133–140 (2010).
17. Taniguchi, H. *et al. Neuron* **71**, 995–1013 (2011).
18. Isaacson, J.S. & Scanziani, M. *Neuron* **72**, 231–243 (2011).
19. Gentet, L.J. *et al. Nat. Neurosci.* **15**, 607–612 (2012).
20. Lee, S.-H. *et al. Nature* **488**, 379–383 (2012).

ONLINE METHODS

Mice. Experiments were conducted in accordance with the ethical guidelines of the US National Institutes of Health and with the approval of the Institutional Animal Care and Use Committee of the University of Pennsylvania. *loxP*-flanked *Mecp2*$^{2lox/+}$ (ref. 6), *Mecp2*$^{Stop/+}$ (ref. 14), *Dlx5/6-cre*[7], *Emx1-cre*[8], *D1-cre*[11], *D2-cre*[11], *Pvalb-cre*[16], *Sst-cre*[17] mice were all obtained from Jackson Laboratories. All mice were housed in a standard 12-h light:12 h dark cycle with access to ample amounts of food and water. All experiments described were performed using mice on a congenic C57BL/6 background.

Surgical procedures. Each mouse was deeply anesthetized (1–2% isoflurane, vol/vol) and mounted in a stereotaxic frame with non-puncturing ear bars. Three stainless steel electrodes, mounted in a single headstage, were aligned to the sagittal axis of the skull. A stainless steel recording electrode was placed 2.0 mm posterior, 2.0 mm left lateral relative to bregma and 1.8 mm depth. Ground and reference electrodes were placed anterior of the hippocampal electrode at 1.0 mm and 2.0 mm distances, respectively. The headstage was then fixed to the skull with screws with dental acrylic.

Data acquisition and analysis. ERP recordings were performed on freely mobile, non-anesthetized mice in their home cage environment after 20-min acclimation to the recording room at 10-14 weeks of age. For LFP recording, neural signals were acquired using Spike2 software connected to a Power 1401 II interface module (CED) and high-impedance differential AC amplifier (A-M Systems). Signals were amplified (gain: 1,000), filtered (1–500 Hz) and sampled at 1.67 kHz. Auditory stimuli consisting of a series of 250 white-noise pips (10-ms duration, 85-dB SPL, 0.25-Hz frequency). Stimuli were presented through speakers on the recording chamber ceiling (Model 19-318A, 700–10,000-Hz frequency response, RadioShack) connected to a digital audio amplifier (RCA Model STAV3870, RadioShack). Stimuli were calibrated using a sound pressure meter. Due to frequency response of speakers, white noise has a corresponding bandwidth of 700–10,000 kHz. Analysis of event-related power and phase-locking factor (PLF) were performed similar to that described previously[4], except instantaneous power and phase were calculated using wavelet methods with custom C routines. Event-related phase locking was measured using a PLF by calculating 1 – circular variance of instantaneous phase measurements, defined as

$$PLF = 1 - \frac{1}{n}\sqrt{\sum_{k=1}^{n}(\cos\theta_k)^2 + \sum_{k=1}^{n}(\sin\theta_k)^2}$$

Auditory brainstem response (ABR) recordings were performed using the same equipment and electrode placement as other recordings except EEG signals were acquired at 15.6 kHz. Auditory stimulation consisted of 4,000 white-noise pips (3-ms duration, 8-Hz frequency) at 85-, 80-, 75-, 70-, 65-, 60- and 55-dB SPL. LFP signal was digitally filtered between 100 and 500 Hz and EEG amplitudes averaged across trials centered at t = 0 s representing sound presentation.

For statistical analysis, event-related power and PLF were separated into frequency ranges with the mean power or PLF calculated between frequencies: δ, 2–4 Hz; θ, 4–8 Hz; α, 8–12 Hz; β, 12–30 Hz; γ_{low}, 30–50 Hz; γ_{high}, 50–90 Hz; ε, 90–140 Hz. Statistical significance was assessed using permutation tests based on t statistics and false discovery correction made using the q-value methodology as previously described[21].

Animal behavior. All animal behavioral studies were carried out blinded to genotype. Mice were allowed to habituate to the testing room for at least 30 min before the test and testing was performed at the same time of day. All animal behaviors were performed on adult male littermates at 12–15 weeks of age.

Phenotypic scoring. Mice were scored for the absence or presence of RTT-like symptoms as described previously[14]. This test provides a semiquantitative assessment of symptom status. Each of six symptoms was scored as 0 (absent or as wild type), 1 (symptom present) or 2 (symptom severe). Symptoms assessed were mobility, gait, hindlimb clasping, tremor, breathing and overall condition. Symptoms were scored as previously described[14]. Mice were also weighed at each scoring session. Statistics were calculated using two-way ANOVA (genotype × phenotypic score) with Bonferroni's *post hoc* analysis.

Elevated zero maze. The elevated zero maze (Stoelting) consists of a circular-shaped platform elevated above the floor. Two opposite quadrants of the maze are enclosed (wall height, 12 inches), whereas the other two are open (wall height, 0.5 inches). Mice were placed in one of the closed quadrants and their movement traced over the course of 5 min. Analysis was performed with automated tracking software (TopScan software, Clever Systems). Statistics were performed using unpaired two-tailed t test with Welch's correction to assume unequal variances.

Open field. Activity in an open field was quantified in a Plexiglas open-field box (43 × 43 cm^2) with two sets of 16 pulse-modulated infrared photobeams (MED Associates). Data were analyzed based on total distance traveled and time spent in two zones: center (25% total area) and surround (75% total area). Statistics were performed using unpaired two-tailed t test with Welch's correction to assume unequal variances.

Accelerating rotarod. Mice were placed on an accelerating rotarod apparatus (Med Associates) for 16 trials (4 trials a day on 4 consecutive days) with at least 15 min of rest between the trials. Each trial lasted for a maximum of 5 min, during which the rod was linearly accelerated from 3.5 to 35 rpm. The amount of time for each mouse to fall from the rod was recorded for each trial. Statistics were calculated using two-way ANOVA (genotype × trial).

Three-chamber social test. The three-chamber social test was conducted as described[22]. The test mice were introduced into the center chamber of the three-chambered apparatus and allowed to acclimate for 10 min. In the social choice test, a novel juvenile male (3–4 weeks of age, A/J mouse, Jackson Laboratory) was introduced to the 'social' chamber, inside a transparent Plexiglas cylinder containing multiple holes to allow for air exchange. In the other (nonsocial) chamber, a paperweight was placed in an identical empty cylinder. During the novel social test, a novel age-matched conspecific male mouse was introduced to the 'novel' chamber, inside a cylinder as before. In the other (familiar) chamber, a cage mate control (whom the test mouse had been housed with since weaning) was placed in an identical cylinder. The designations of the social and nonsocial chambers or novel and familiar chambers were randomly chosen in each test to prevent chamber bias. Between tests, the chambers were cleaned with water and allowed to dry completely before initiating the next test. The time spent interacting (sniffing, climbing) the cylinders was quantified using automated tracking software (TopScan software, Clever Systems). Statistics were calculated using two-way ANOVA (genotype × trial).

Fear conditioning. The fear-conditioning apparatus consisted of a conditioning cage (16 × 6 × 8 inches) with a grid floor wired to a shock generator and a scrambler, surrounded by an acoustic chamber. To induce fear conditioning, mice were placed in the cage for 120 s, and then a pure tone (2 kHz) was played for 20 s, followed by a 2-s foot shock (0.75 mA). Immediate freezing behavior was monitored for a period of 60 s, followed by a second tone and shock and freezing measurement taken once again for 60 s. Mice were then returned to their home cage. Fear conditioning was assessed 24 h later by a continuous measurement of freezing (complete immobility). To test contextual fear conditioning, mice were placed in the original conditioning cage and freezing was measured for 5 min. To test auditory-cued fear conditioning, mice were placed in a different context: the walls of the conditioning cage were altered, the floor grid covered and cage scented with almond. As a control for the influence of the novel environment, freezing was measured for 2 min in this new environment, and then a 2-kHz tone was played for 1 min, during which conditioned freezing was measured. Statistics were calculated using two-way ANOVA (genotype × test).

Immunohistochemistry. Mice were deeply anesthetized (Avertin, 250 mg per kg of body weight), perfused with 4% paraformaldehyde (wt/vol) in 0.1 M sodium-potassium phosphate buffered saline, and 20-μm coronal or sagittal sections taken. Immunohistochemistry was performed on free-floating sections as previously described[4] with mouse antibody to GAD67 (1:500, Millipore), mouse antibody to PV (1:500, Millipore) and a custom rabbit antibody to MeCP2 (1:1,000)[23]. All immunohistochemistry experiments were successfully repeated in three different mice per genotype.

Statistics. Data are presented as mean ± s.e.m. Statistical analyses were performed using GraphPad Prism software unless otherwise stated. Data distribution was assumed to be normal, but this was not formally tested. Furthermore, variance was found to be similar between groups being statistically compared. No statistical methods were used to pre-determine sample sizes, but our sample sizes are similar to those reported in previous publications[4,22]. For all experiments, the experimenter was blind to genotype and samples were pseudo-randomized. No animals were excluded from analyses. A **Supplementary Methods Checklist** is available.

21. Storey, J.D. & Tibshirani, R. *Proc. Natl. Acad. Sci. USA* **100**, 9440–9445 (2003).
22. Wang, I.-T.J. *et al. Proc. Natl. Acad. Sci. USA* **109**, 21516–21521 (2012).
23. Zhou, Z. *et al. Neuron* **52**, 255–269 (2006).

doi:10.1038/nn.3710

SUPPLEMENTARY INFORMATION

Cellular Origins of Auditory Event-Related Potential Deficits in Rett Syndrome

Darren Goffin, Edward S. Brodkin, Julie A. Blendy, Steve J. Siegel and Zhaolan Zhou*

*Correspondence: zhaolan@mail.med.upenn.edu

This PDF file includes:

Supplementary Figures 1 to 10

Captions for Supplementary Movies 1 to 4

Other Supplementary Materials for this manuscript includes the following:

Supplementary Movies 1 to 4

Nature Neuroscience: doi:10.1038/nn.3710

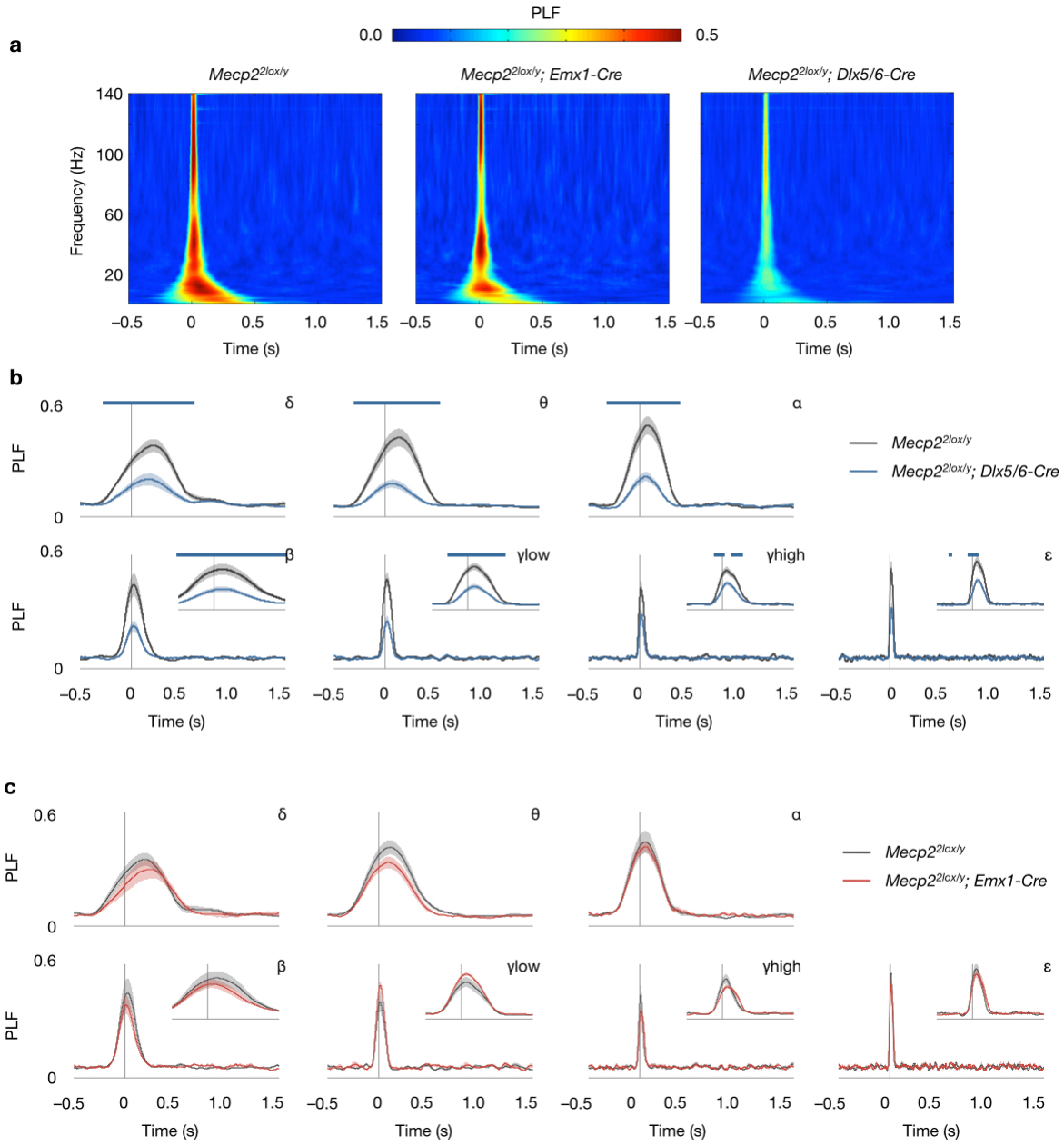

Supplementary Figure 1 Auditory evoked phase-locking factor (PLF) responses following loss of MeCP2 from forebrain GABAergic or glutamatergic neurons. (**a**) Heat maps showing changes in event-related PLF in response to 85-dB white noise sound presentation as a function of time and frequency. (**b**) Population averages of event-related power separated into frequency bands (δ, 2-4 Hz; θ, 4-8 Hz; α, 8-12 Hz; β, 12-30 Hz; γlow, 30-50 Hz; γhigh, 50-90 Hz; ε, 90-140 Hz) for *Mecp2$^{2lox/y}$; Dlx5/6-Cre* mice (n = 13) and their wild-type (*Mecp2$^{2lox/y}$*) littermates (n = 9). (**c**) Population averages for *Mecp2$^{2lox/y}$; Emx1-Cre* mice (n = 7) and their *Mecp2$^{2lox/y}$* littermates (n = 7). Shaded regions represent s.e.m. Top blue bars represent those regions with an FDR < 0.05 (permutation test).

Nature Neuroscience: doi:10.1038/nn.3710

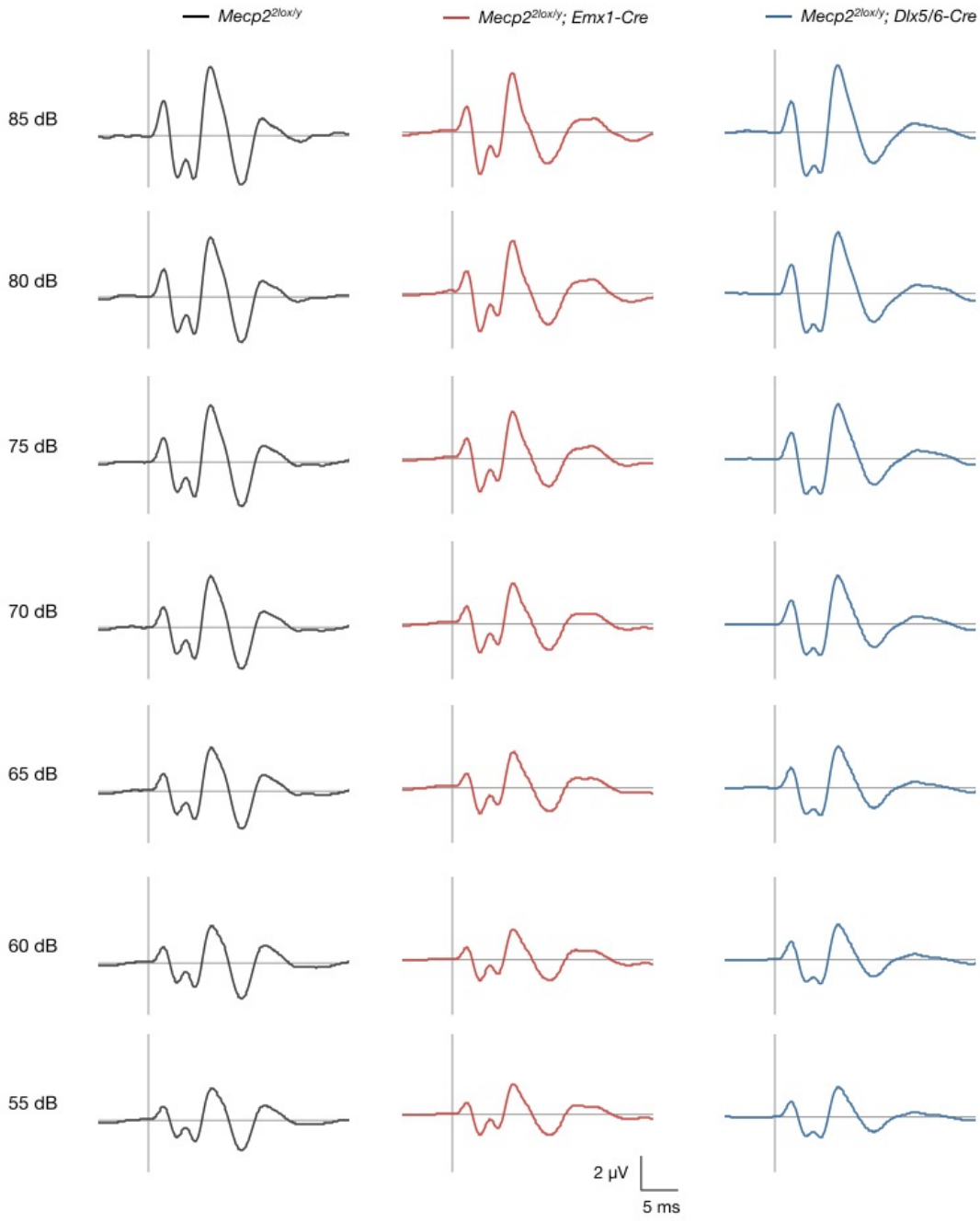

Supplementary Figure 2 Auditory brainstem responses are not affected following deletion of MeCP2 from forebrain GABAergic or glutamatergic neurons. Auditory brain stem responses (ABR) from *Mecp2$^{2lox/y}$*, *Mecp2$^{2lox/y}$; Emx1-Cre* and *Mecp2$^{2lox/y}$; Dlx5/6-Cre* mice. ABR responses decreased to a similar extent in all three genotypes with decreasing sound pressure.

Nature Neuroscience: doi:10.1038/nn.3710

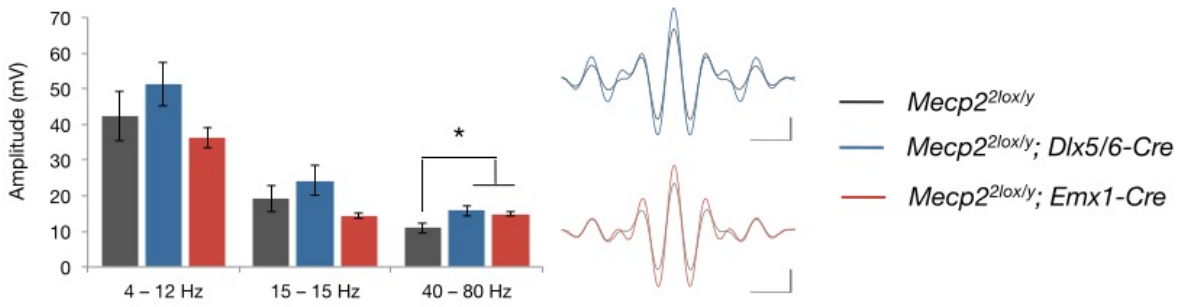

Supplementary Figure 3 Elevated high frequency oscillations following conditional deletion of MeCP2 from forebrain GABAergic or glutamatergic neurons. Basal EEG power measurements in *Mecp2$^{2lox/y}$; Dlx5/6-Cre* mice (n = 13), *Mecp2$^{2lox/y}$; Emx1-Cre* mice (n = 7) mice and their wild-type (*Mecp2$^{2lox/y}$*) littermates (n = 9). Insets show 40-80 Hz mean amplitudes across EEG recordings. Scale bars represent one oscillation cycle (horizontal) and 20 μV (vertical). Bars represent mean ± s.e.m. *P < 0.05, two-tailed t-test with Bonferroni correction.

Nature Neuroscience: doi:10.1038/nn.3710

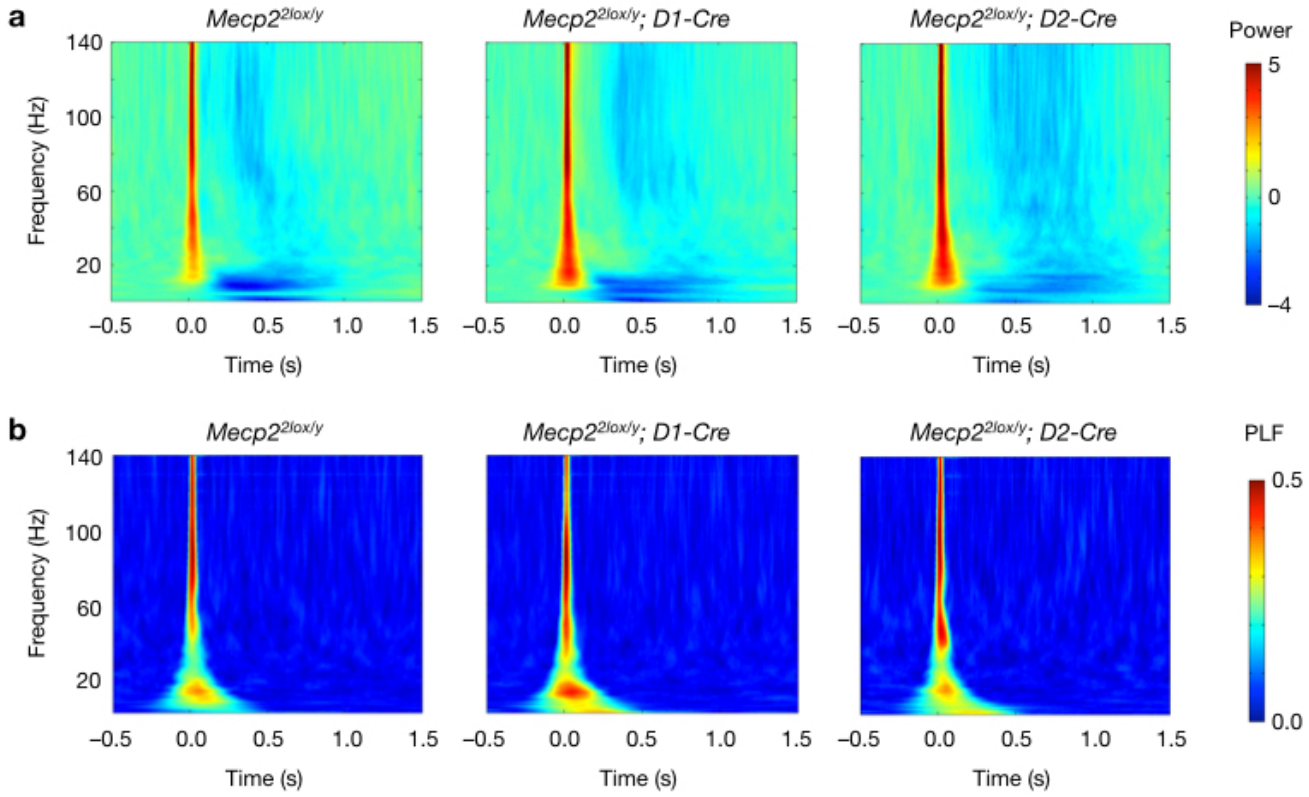

Supplementary Figure 4 Event-related power or PLF are not affected by loss of MeCP2 from D1- or D2-dopamine receptor-expressing medium spiny neurons. Heat maps showing changes in event-related power (**a**) or PLF (**b**) in response to 85-dB white noise sound presentation as a function of time and frequency in *Mecp2$^{2lox/y}$; D1-Cre* mice (n = 9), *Mecp2$^{2lox/y}$; D2-Cre* mice (n = 10) and wild-type (*Mecp2$^{2lox/y}$*) littermates (n = 9).

Nature Neuroscience: doi:10.1038/nn.3710

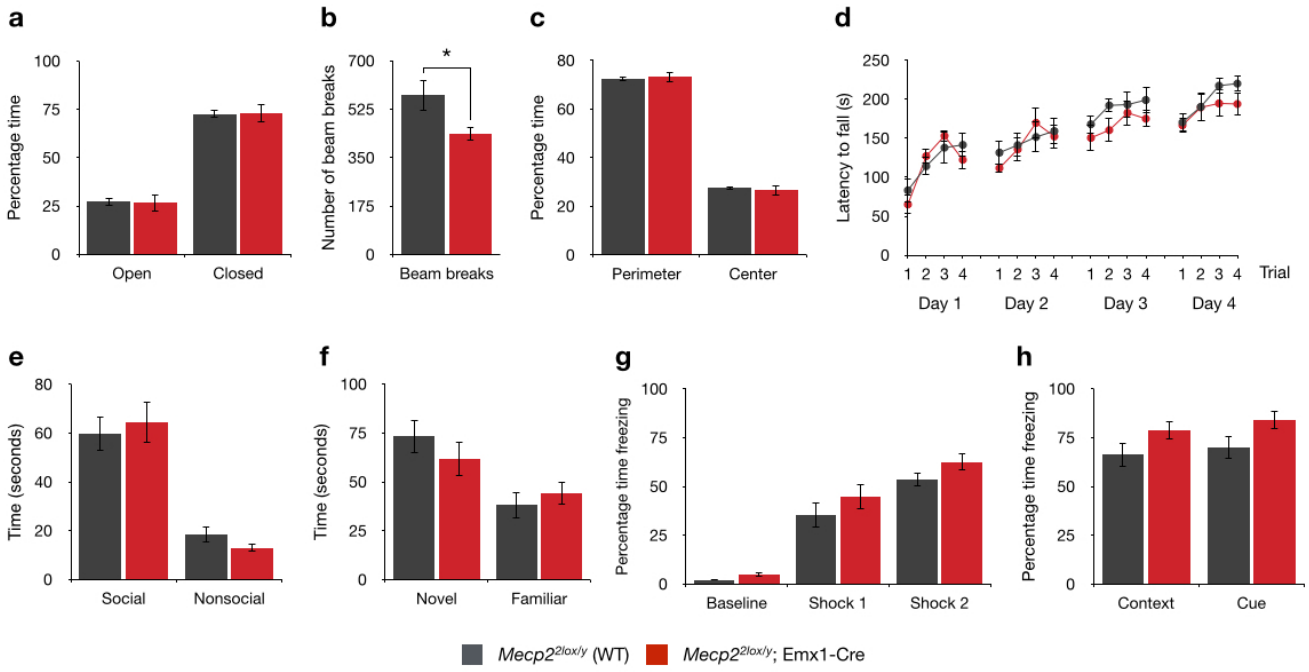

Supplementary Figure 5 Behavioral analysis of mice lacking MeCP2 in forebrain glutamatergic neurons. (**a**) Percentage time spent in open and closed regions of elevated zero maze ($p = 0.50$). (**b**) Number of beam breaks across 5 minutes of open field assay ($p = 0.043$). (**c**) Percentage time spent in center and periphery of open field assay ($p = 0.50$). (**d**) Latency to fall from accelerating rotarod ($F[1, 272] = 3.70$, $p = 0.056$, genotype). (**e**) Social approach towards a social (mouse) versus a nonsocial object in a three-chamber test ($F[1, 14] = 0.02$, $p = 0.89$, genotype). (**f**) Social approach behavior towards a novel mouse versus a familiar cage mate control mouse in a three-chamber test ($F[1, 12] = 0.78$, $p = 0.40$, genotype). (**g**) Time spent freezing during fear-conditioning training following foot shocks ($F[1, 51] = 1.57$, $p = 0.22$, genotype). (**h**) Time spent freezing in response to context or cue 24 hours following training ($F[1, 34] = 3.11$, $p = 0.09$, genotype). Bars represent mean ± s.e.m. Statistics were performed using two-way ANOVA or an unpaired two-tailed t-test with Welch's correction. Behavioral experiments were performed at 13-15 weeks of age (n = 9 for *Mecp2$^{2lox/y}$; Emx1-Cre* mice and n = 10 for wild-type, *Mecp2$^{2lox/y}$* littermates).

Nature Neuroscience: doi:10.1038/nn.3710

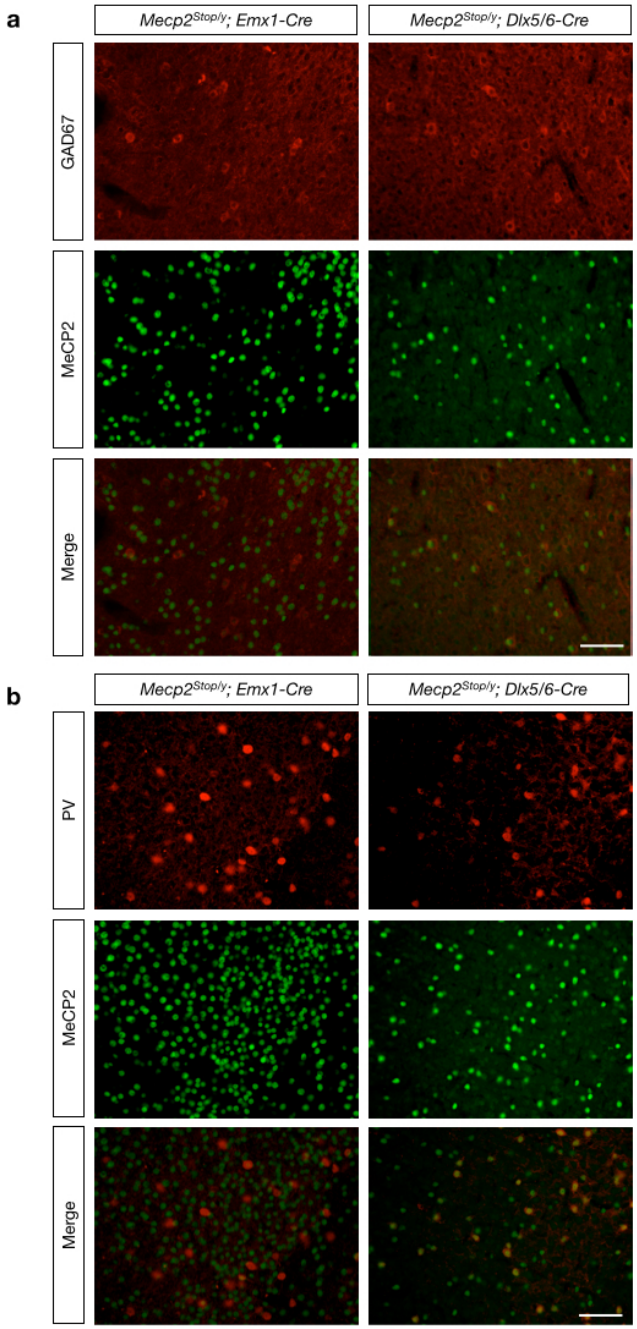

Supplementary Figure 6 Preservation of MeCP2 expression in GAD67- and PV-expressing interneurons in *Mecp2*$^{Stop/y}$*; Dlx5/6-Cre* but not *Mecp2*$^{Stop/y}$*; Emx1-Cre* mice. Representative images showing MeCP2 expression in cortex and its co-localization with GAD67 (**a**) or Parvalbumin (**b**). Scale bars correspond to 75 μm. MeCP2 immunoreactivity is absent from GAD67- and PV-expressing neurons in *Mecp2*$^{Stop/y}$*; Emx1-Cre* mice. In contrast, MeCP2 expression is preserved in GAD67-and PV-expressing neurons in *Mecp2*$^{Stop/y}$*; Dlx5/6-Cre* mice. These localization patterns were observed in three mice per genotype.

Nature Neuroscience: doi:10.1038/nn.3710

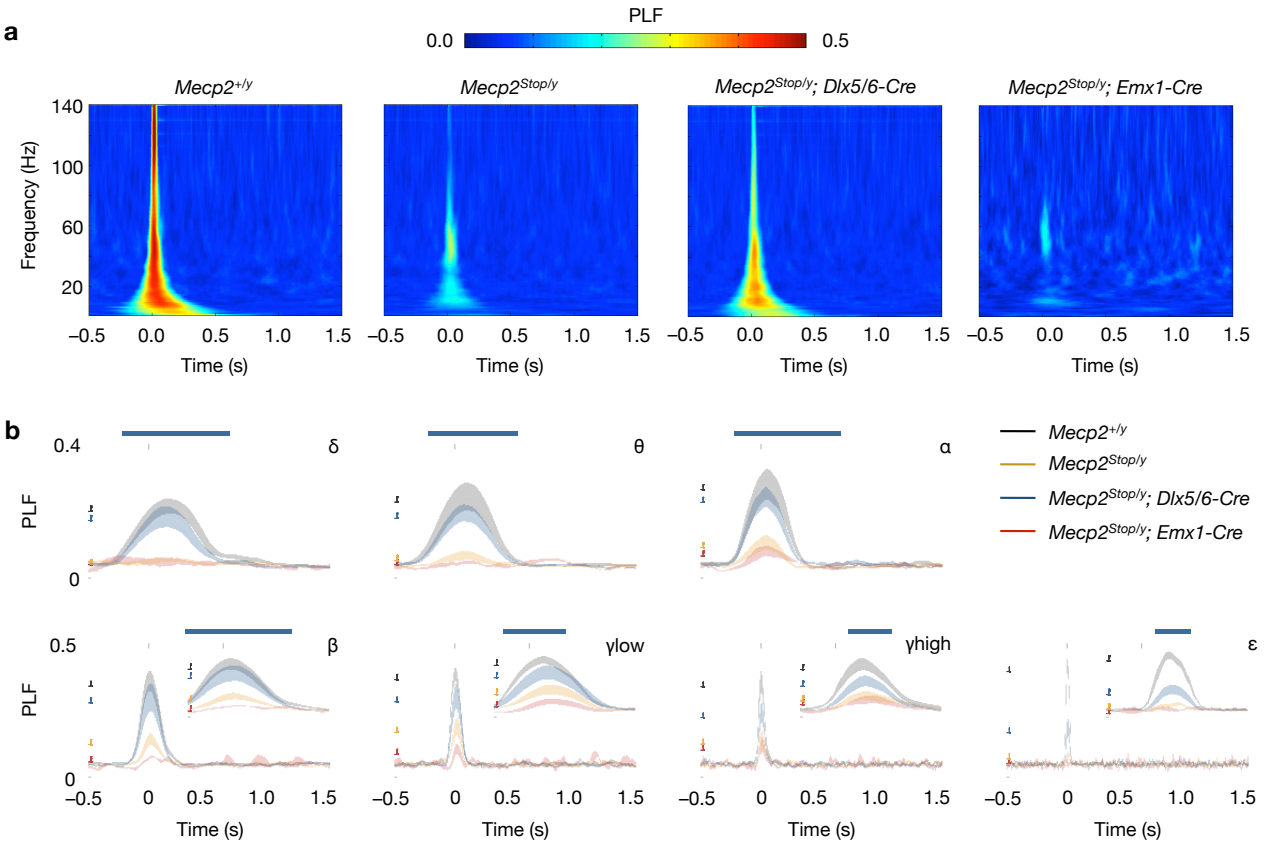

Supplementary Figure 7 Amelioration of PLF deficits following preservation of MeCP2 expression in forebrain GABAergic but not glutamatergic neurons. (**a**) Heat maps showing changes in event-related PLF in response to 85-dB white noise sound presentation as a function of time and frequency. (**b**) Population averages of event-related power separated into frequency bands (δ, 2-4 Hz; θ, 4-8 Hz; α, 8-12 Hz; β, 12-30 Hz; γlow, 30-50 Hz; γhigh, 50-90 Hz; ε, 90-140 Hz) for *Mecp2*$^{Stop/y}$*; Dlx5/6-Cre* mice (n = 11), *Mecp2*$^{Stop/y}$*; Emx1-Cre* mice (n = 6), *Mecp2*$^{Stop/y}$ mice (n = 9) and WT littermates (n = 9). Shaded regions represent s.e.m. Top blue bars represent those regions with an FDR < 0.05 (permutation test).

Nature Neuroscience: doi:10.1038/nn.3710

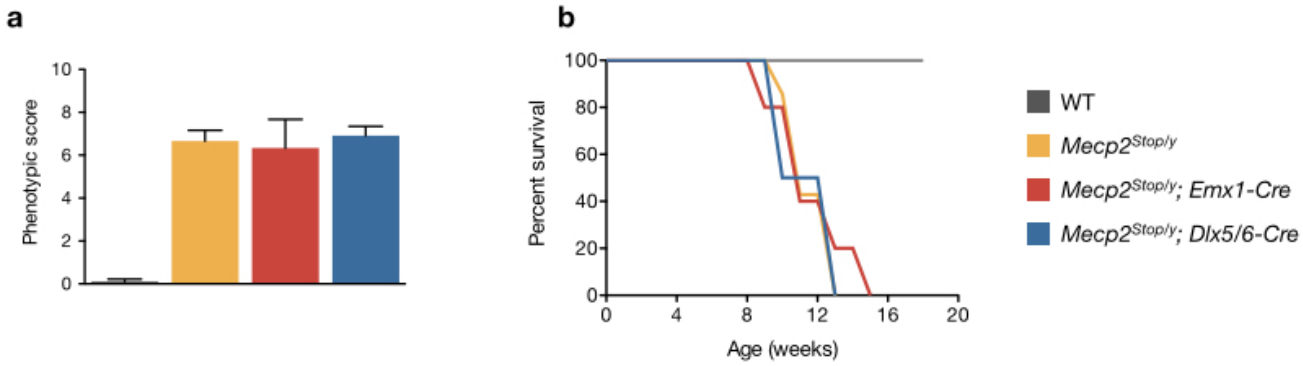

Supplementary Figure 8 Overt RTT-like phenotypes and premature lethality are not ameliorated by preservation of MeCP2 expression in forebrain GABAergic or glutamatergic neurons. (**a**) Phenotypic scoring of RTT-like phenotypes in mice at 12 weeks of age (n = 7 per genotype). Statistics performed using one-way ANOVA with Tukey post-test analysis ($F(2,18) = 0.13$, $p = 0.88$, genotype). (**b**) Longevity of mice with indicated genotypes (n = 7 per genotype).

Nature Neuroscience: doi:10.1038/nn.3710

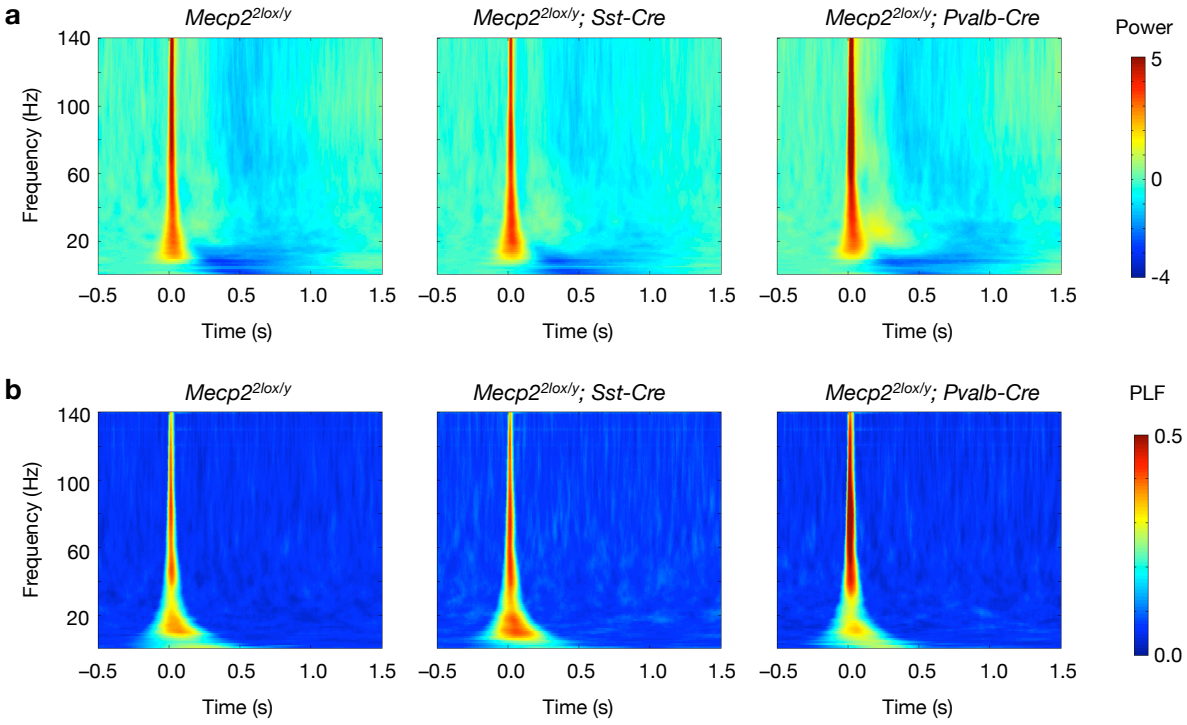

Supplementary Figure 9 Event-related power or PLF are not affected by loss of MeCP2 from PV- or SOM-expressing interneurons. Heat maps showing changes in event-related power (**a**) or PLF (**b**) in response to 85-dB white noise sound presentation as a function of time and frequency in *Mecp2*$^{2lox/y}$*; Sst-Cre* mice (n = 14), *Mecp2*$^{2lox/y}$*; Pvalb-Cre* mice (n = 10) and wild-type *Mecp2*$^{2lox/y}$ littermates (n = 12).

Nature Neuroscience: doi:10.1038/nn.3710

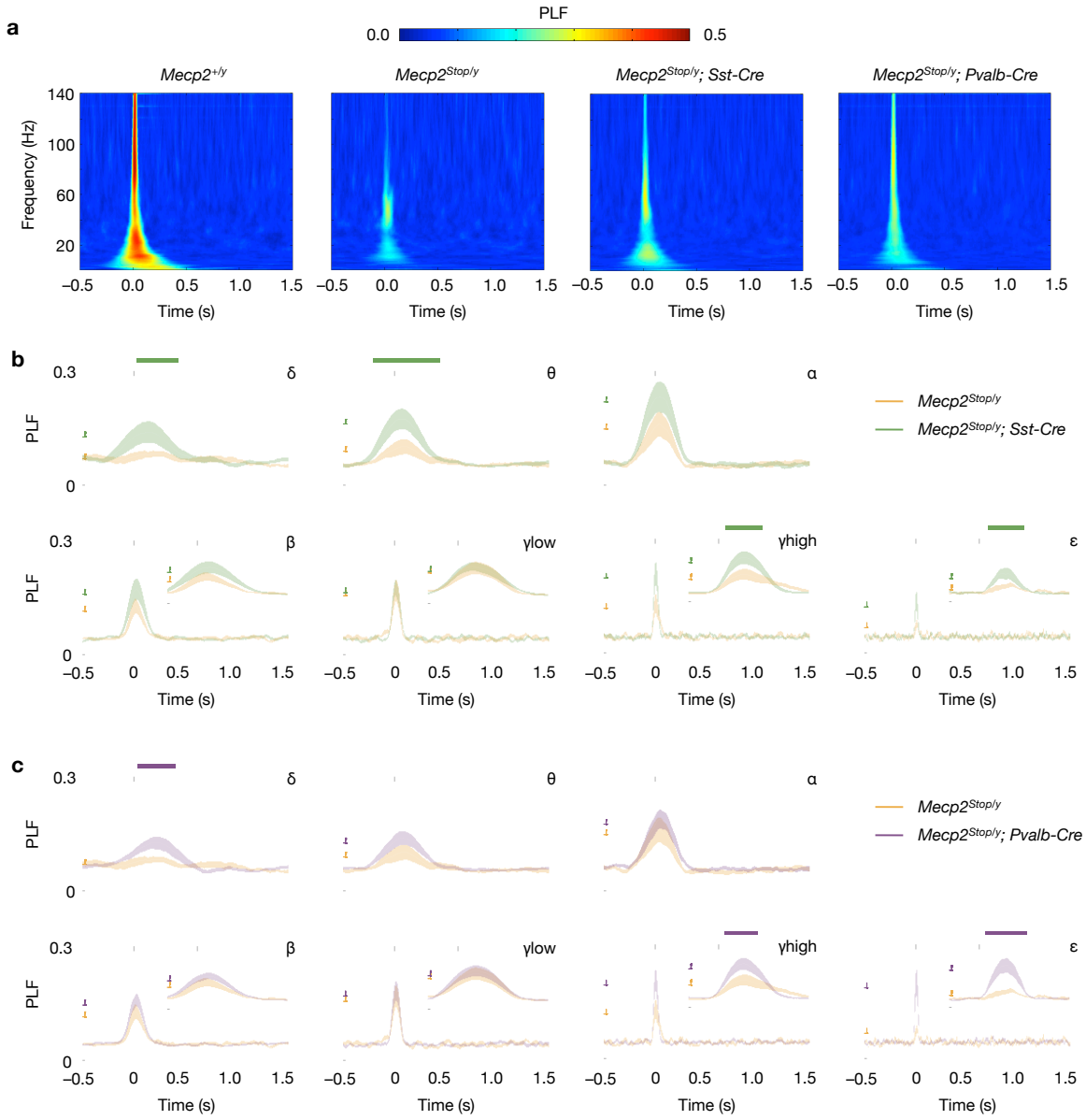

Supplementary Figure 10 Amelioration of PLF deficits following preservation of MeCP2 expression in PV- or SOM-expressing interneurons. (**a**) Heat maps showing changes in event-related PLF in response to 85-dB white noise sound presentation as a function of time and frequency. (**b**) Population averages of event-related power separated into frequency bands (δ, 2-4 Hz; θ, 4-8 Hz; α, 8-12 Hz; β, 12-30 Hz; γlow, 30-50 Hz; γhigh, 50-90 Hz; ε, 90-140 Hz) for *Mecp2*$^{Stop/y}$*; Pvalb-Cre* mice (n = 7) and *Mecp2*$^{Stop/y}$ mice (n = 9). (**c**) Population averages for *Mecp2*$^{Stop/y}$*; Sst-Cre* (n = 12) and *Mecp2*$^{Stop/y}$ mice (n = 9). Shaded regions represent s.e.m. Top line represents those regions with an FDR < 0.05 (permutation test).

Nature Neuroscience: doi:10.1038/nn.3710

Supplementary Movie 1

A behavioral seizure observed in an *Mecp2*$^{2lox/y}$*; Dlx5/6-Cre* mouse.

Supplementary Movie 2

A behavioral seizure observed in another *Mecp2*$^{2lox/y}$*; Dlx5/6-Cre* mouse.

Supplementary Movie 3

A seizure leading to bubbling liquid at mouth in an *Mecp2*$^{2lox/y}$*; Dlx5/6-Cre* mouse.

Supplementary Movie 4

A behavioral seizure observed in an *Mecp2*$^{Stop/y}$*; Emx1-Cre* mouse.

Nature Neuroscience: doi:10.1038/nn.3710